Effects of Stearyl Alcohol Monolayer on the Structure, Dynamics and Vibrational Sum Frequency Generation Spectroscopy of Interfacial Water

Supplementary Information

Banshi Das and Amalendu Chandra*

Department of Chemistry, Indian Institute of Technology Kanpur, Uttar Pradesh, India 208016.

*E-mail: amalen@iitk.ac.in, Tel: +91 512 2597241

1 Effects of stearyl alcohol (STA) force field

In order to investigate the effects of force field of STA molecules on the calculated orientational profiles and VSFG spectrum of interfacial water, we also calculated the partial charges of STA molecules with the B3LYP functional[1–3] and 6-311++G** basis set by using the Gaussian 09 program[4] in addition to doing such calculations at the Hartree-Fock level with the 6-31G* basis set. Subsequently, we performed molecular dynamics simulation of the STA-water interface with the B3LYP/6-311++G** partial charges of STA and SPC/E model of water by following the same simulation protocol as described in Sec. 2.1. The orientational profiles show the distributions of the angles that OH bonds of interfacial water molecules makes with the surface normal. We have used the commonly used 90%-10% definition of the interface as described in Sec.3.1 to identify the interfacial molecules for calculation of the orientational distributions. Both the calculated orientational distributions and VSFG spectra from the two simulations are found to be very similar (Figures S1a and S1b).

2 Structural properties

The conventional spherical radial distribution functions are not appropriate for describing arrangement of atoms for the interfacial systems considered here. Due to anisotropy of the interfaces along the z-direction, we have calculated the slab radial distribution functions (SRDF) by considering xy-slabs of thickness 4 Å and the position of the reference water molecule is taken to be at the center of the chosen slab. Each SRDF is then normalized by the average water density for that particular slab. The results of SRDFs are shown in Figure S2. In order to have further insights into the structure of interfaces, we have also calculated the density profiles of water using the method of instantaneous water surface[5] and the results are shown in Figure S3. The instantaneous density profiles also reveal a narrower interface for the STA-water system than the TBA-water interface. The results of both Figures S2 and S3 are for the HF/6-31G* partial charges of STA and SPC/E model of water.

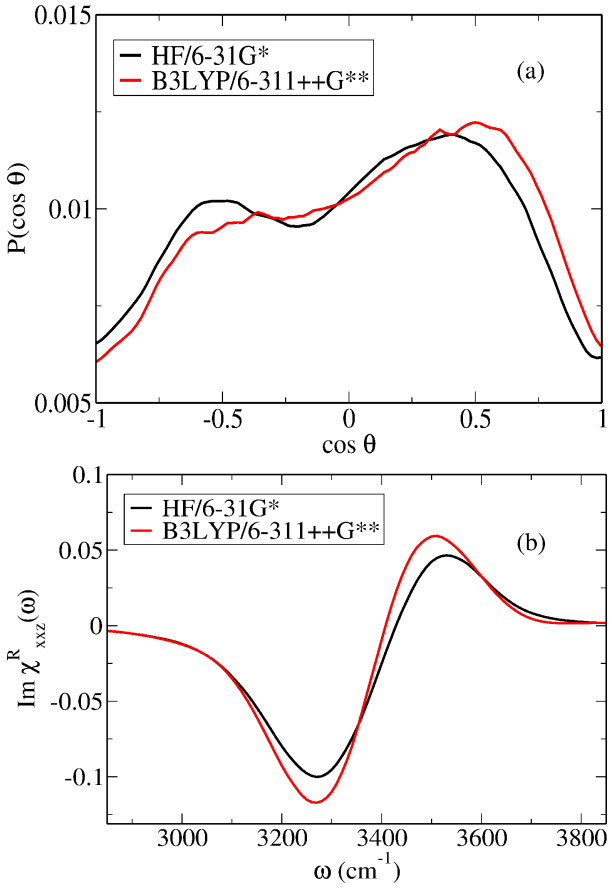

Figure S1: (a) Orientational distributions of OH bonds of interfacial water and (b) calculated VSFG spectrum for STA-water system with two different sets of partial charges on different atoms of STA molecules as obtained from quantum chemical calculations at two different levels. The angle θ represents the angle of an OH bond of interfacial water with respect to the surface normal. The results are for the SPC/E model of water.

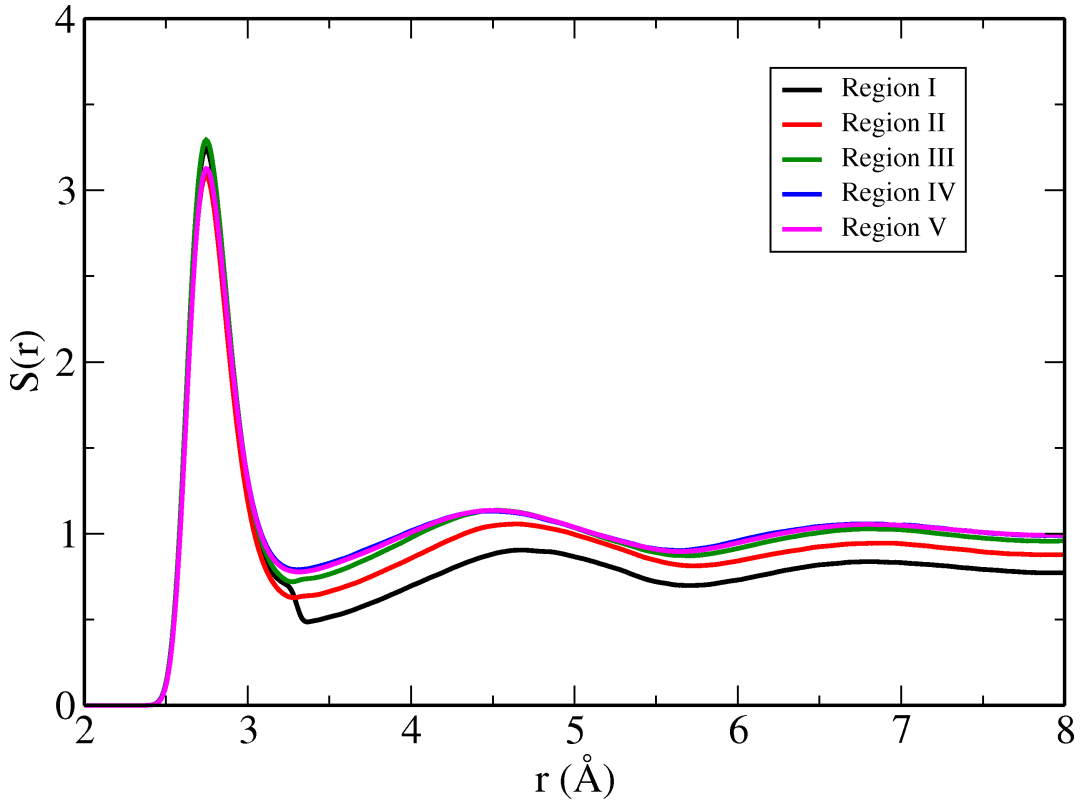

Figure S2: Slab radial distribution functions for different regions (I-V) of the stearyl alcohol-water interfacial system. The results are for HF/6-31G* and SPC/E force fields for STA and water, respectively.

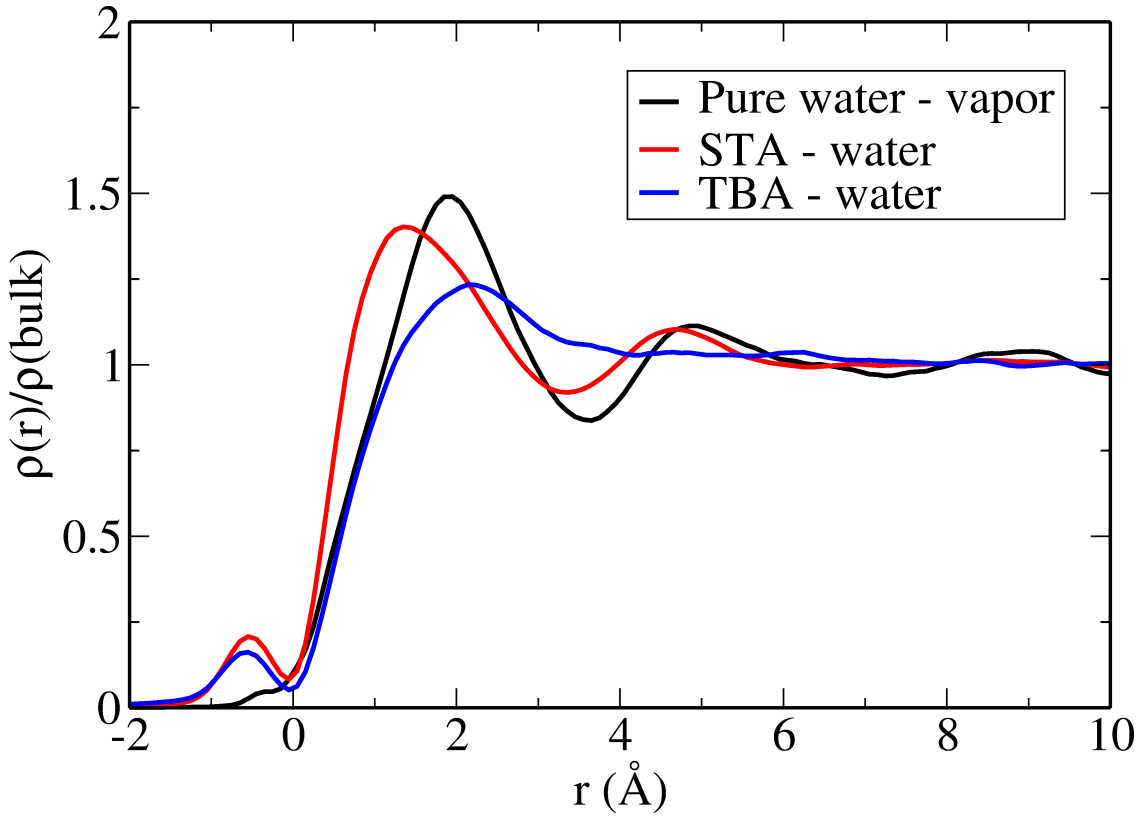

Figure S3: Mean relative density profiles with respect to the distance (r) from the instantaneous interface. The results are for HF/6-31G* and SPC/E force fields for STA and water, respectively.

3 Orientational distributions and imaginary $\chi^{(2)}$ spectrum of the STA-water interface for TIP4P/2005 water model

In order to calculate the interfacial structure and VSFG spectrum for another water model, we have considered the TIP4P/2005 model[6] of water and carried out simulations using both the HF/6-31G* and B3LYP/6-311++G** force field parameters of STA as described in Sec. 2.1. We calculated the frequency mapping relationships for spectral calculations for this water model by extracting 500 clusters from a 10 ns simulation of a bulk system with 256 TIP4P/2005 water molecules and performing quantum chemical calculations using the procedure as described earlier[7]. Specifically, we used the B3LYP functional and 6-311++G** basis set for the electronic structure calculations to establish the mapping relations specific to the TIP4P/2005 water model (Table S1).

In Figure S4, we have shown the orientational distributions and imaginary VSFG spectrum of interfacial water for the TIP4P/2005 model for both force field parameters of STA. As can be seen, the orientational distributions and the VSFG spectrum are rather similar for the two STA force fields considered here. In Figure S5, we have compared the results of orientational distributions and imaginary VSFG spectra of TIP4P/2005 and SPC/E models for the HF/6-31G* force field of STA. The orientational distributions of the two water models are found to be rather similar. However, the imaginary part of $\chi^R_{\mathrm{xxz}}(\omega)$ of the STA-water interface seems to exhibit some differences for the two water models (Figure S5b). For example, the negative region of the imaginary $\chi^R_{\mathrm{xxz}}(\omega)$ spectrum for TIP4P/2005 model appears at a higher frequency than SPC/E and also the TIP4P/2005 shows a mild positive peak at $\sim 3350\,\mathrm{cm}^{-1}$ which is not exhibited by the SPC/E model.

In order to decipher the origin of this difference, we deconvoluted the total imaginary $\chi^R_{\mathrm{xxz}}(\omega)$ response for the TIP4P/2005 model into contributions from different regions as defined in Sec. 3.1. The responses from different regions (Figure S6) are found to be qualitatively similar to those for the SPC/E model (Figure 2) in the sense that major contributions to the $\chi^R_{\mathrm{xxz}}(\omega)$ spectrum come from interfacial regions I and II, although their relative peak positions are not the same for the two models. Subsequently, following Ref. [8], we divided the interfacial water molecules into three categories of $\mathrm{W_D}$, $\mathrm{W_A}$ and $\mathrm{W_{WAT}}$, where $\mathrm{W_D}$ corresponds to water molecules which donate hydrogen bonds to the alcohol

molecules, W_A corresponds to water molecules which accept hydrogen bonds from the alcohol molecules, and W_{WAT} corresponds to water molecules which do not form hydrogen bonds with any alcohol molecule. In Figures S7 and S8, we have shown the contributions of W_D, W_A and WAT molecules to the VSFG spectrum for SPC/E and TIP4P/2005 water models, respectively. The spectral responses from these three categories of water molecules for the two models are found to be qualitatively similar in the sense that the W_D molecules make net positive and W_A molecules make net negative contributions to the imaginary $\chi^R_{xxz}(\omega)$ spectrum which is consistent with their average orientations. Qualitatively, similar results were also found earlier for the calculated imaginary χ^R_{xxz} spectrum of alcohol-water interfaces[8]. However, the relative positions of the W_D and W_A peaks along the frequency axis are found to be different for the two water models. While the W_D peak appears at a higher frequency than the W_A peak for the SPC/E model, it is opposite for the TIP4P/2005 model. In fact, the relative positions of the W_D and W_A peaks for the TIP4P/2005 model appear to be similar to that of Ref.[8] where also the simulation trajectories were generated using the rigid TIP4P/2005 and flexible q-TIP4P/F[9] models. Since the total spectrum includes the sum of contributions from W_D and W_A with opposite signs, any changes in their relative peak positions can affect the overall imaginary $\chi^{(2)}(\omega)$ spectrum as seen in Figures S7 and S8. Thus, the differences between the calculated imaginary χ^R_{xxz} spectrum of the alcohol-water interface of the current work (SPC/E model) and of Ref.[8] are believed to arise from different water models used in the calculations, rather than from different force fields of the alcohol molecules. We also note in this context that heterodyne experiments of similar alcohol-water interfaces exhibit a single negative peak for the imaginary $\chi^{(2)}(\omega)$ spectrum[10].

Table S1: Empirical relationships of spectral maps for TIP4P/2005 water.

$\omega = 3839.58\ \text{cm}^{-1} - (7116.88\ \text{cm}^{-1}/\text{au})E - (85465.4\ \text{cm}^{-1}/\text{au}^2)E^2$
$x_{10} = 0.1028\ \text{Å} - (0.9319 \times 10^{-5}\ \text{Å}/\text{cm}^{-1})\omega$
$\mu'/\mu'_g = 0.6803 + (77.305\ \text{au}^{-1})E$
$\alpha'/\alpha'_g = 1.1047 + (3.992\ \text{au}^{-1})E$

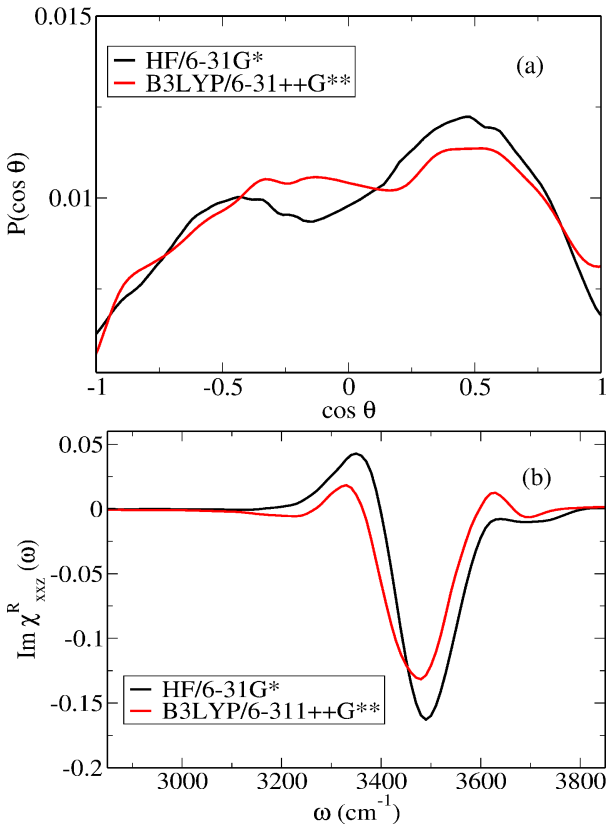

Figure S4: (a) Orientational distributions of OH bonds of interfacial water and (b) calculated VSFG spectrum of STA-water system for TIP4P/2005 water model and two different sets of partial charges of STA molecules. The angle θ represents the angle of an OH bond of interfacial water with respect to the surface normal.

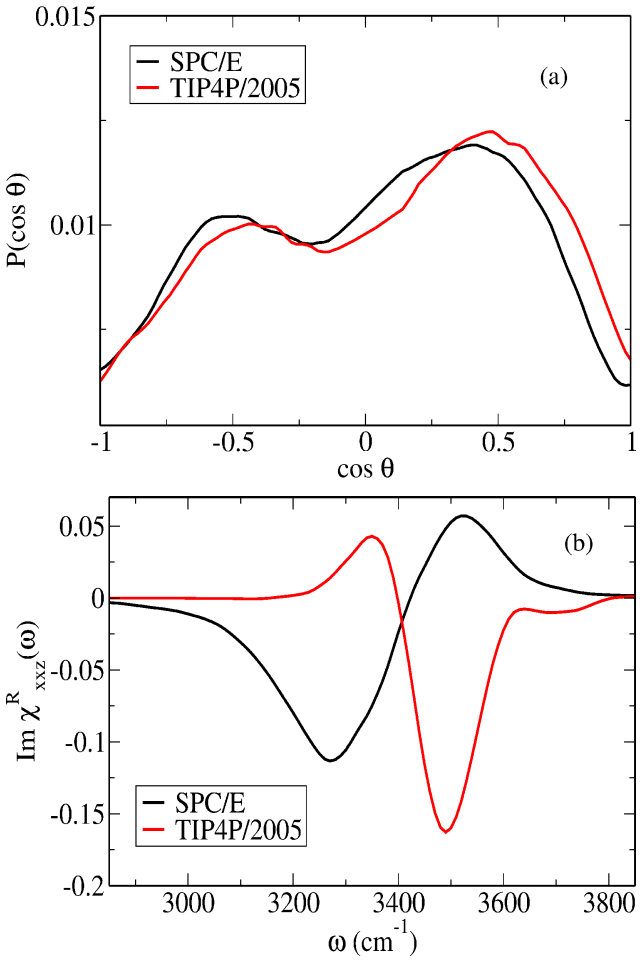

Figure S5: (a) Orientational distributions of OH bonds of interfacial water for the SPC/E and TIP4P/2005 water models. The angle θ represents the angle of an OH bond of interfacial water with respect to the surface normal. The results of this figure and also of the later figures are for HF/6-31G* partial charges of STA.

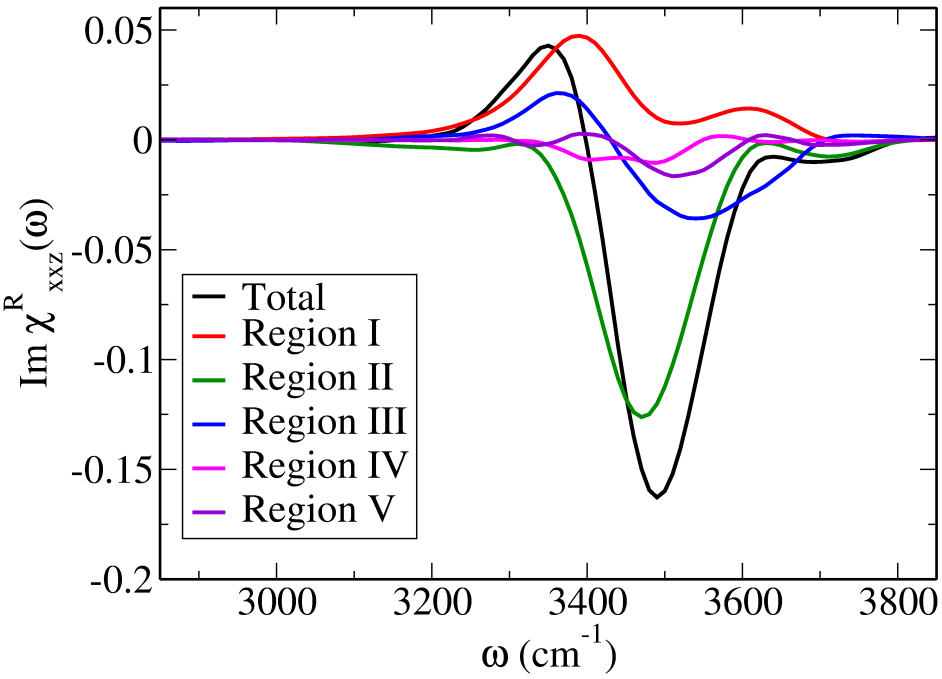

Figure S6: Decomposition of the imaginary $\chi^{R}_{xxz}(\omega)$ spectrum into contributions from different regions (I-V) for the STA-water interface for TIP4P/2005 water model.

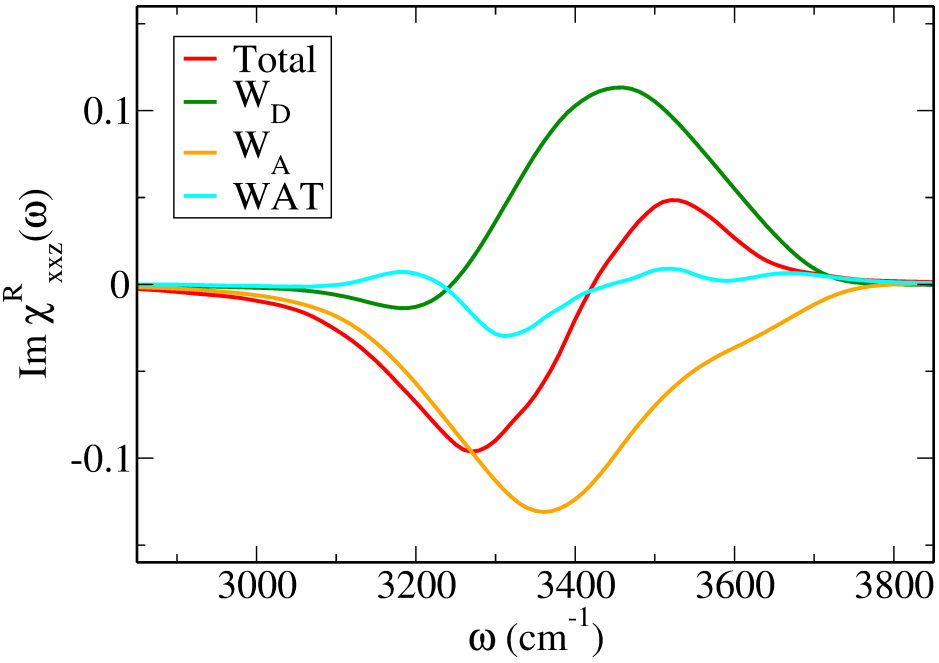

Figure S7: Decomposition of the imaginary $\chi^R_{xxz}(\omega)$ spectrum into contributions from W_D, W_A and WAT molecules of STA-water interface for SPC/E water model.

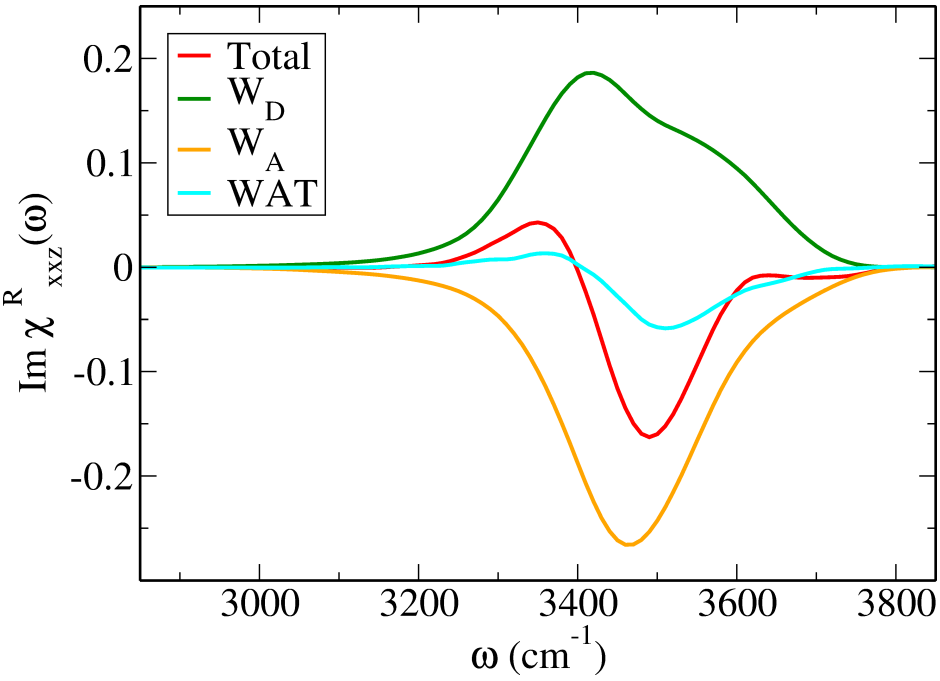

Figure S8: Decomposition of the imaginary $\chi^R_{xxz}(\omega)$ spectrum into contributions from W_D, W_A and WAT molecules of STA-water interface for TIP4P/2005 water model.

4 Intensity of VSFG signals: Comparison of results for SPC/E and TIP4P water models

We have also compared the total VSFG intensity of the STA-water interface for the SPC/E and TIP4P/2005 water models. Generally speaking, apart from resonant $\chi^{(2)}(\omega)$ contribution, the experimentally measured intensity will also have a contribution from nonresonant component. Besides, for interfaces with charged surfaces and/or net polarized dipoles, the VSFG response can also arise from interaction with the static electric field of such charged and/or dipole polarized surfaces[11–14]. The experimentally measured total VSFG intensity, or $|\chi^{(eff)}_{\mathrm{xxz}}|^2$, can then be written in general terms as follows[8]

$$|\chi^{(eff)}_{\mathrm{xxz}}|^2 = |Re\chi^{R}_{\mathrm{xxz}} + \chi^{NR}_{\mathrm{xxz}} - \phi(0)Re\chi^{(3)}_{\mathrm{xxzz}}|^2 + |Im\chi^{R}_{\mathrm{xxz}} - \phi(0)Im\chi^{(3)}_{\mathrm{xxzz}}|^2 \ , \qquad (1)$$

where χ^{NR}_{xxz} is the second order nonresonant background contribution which is approximated to have a real constant value, $\chi^{(3)}_{\mathrm{xxzz}}$ is the third order susceptibility of the bulk phase, and $\phi(0)$ is the electrostatic potential at the Gibbs dividing surface ($z = 0$) produced by the polarized surface moieties. We calculated $\phi(z)$ for the current interfacial system of water covered with STA for the SPC/E model of water by setting the origin of the potential at the centre of the liquid slab in the simulation box and the results are shown in Figure S9a along with that for pure water-air interface. The nature of $\phi(z)$ for the STA-water system is found to be very similar to that of pure water-vapor system. Extrapolating the linear fitting of the bulk $\phi(z)$ part, we found that the surface potential is essentially zero at the interface for the case of STA-water and pure water-vapor systems (Figure S9a), hence the $\chi^{(3)}$ contribution to the VSFG intensity is judged to be negligibly small for the present interfaces and are not included in the subsequent calculations of the intensity. The corresponding results of the surface potential for the TBA-water system for the SPC/E model are also included in Figure S9b for comparison. Note that the results of $\phi(z)$ for TBA-water system are corrected from those reported earlier in the Supporting Information of Reference[7]. Again, $\phi(0)$ is found to be rather small which is not unexpected since the surfaces of these air-water systems with alcohol monolayers are dipolar in nature and do not carry any net charges.

In Figure S10, we have shown the total intensity of VSFG signal for the SPC/E and TIP4P/2005 water models where the nonresonant contribution χ^{NR}_{xxz} is assumed to be 0. The calculated intensities are shown for uncoupled oscillators for the STA-water inter-

face and the corresponding intensities for the pure air-water interface for the respective models are also shown for comparison. As can be seen from this figure, while the SPC/E model shows a red shift of the hydrogen bonded part of the spectrum compared to that of the respective pure air-water spectrum which is in qualitative agreement with the experimental results[15], the TIP4P/2005 model shows essentially the same peak position for the hydrogen bonded part with only a very slight red shift of the corresponding average frequency for the STA-water system. Also, on absolute scale, the peak frequency for the SPC/E model appears to be closer to the experimental peak than the TIP4P/2005 model. In Figure S11, we have shown the calculated results of the VSFG intensity for the STA-water interface for two different values of the nonresonant component (Eq.1 of the Supplementary Information): $\chi^{NR}_{\mathrm{xxz}} = 0$ and -1. The results of this figure are obtained for uncoupled oscillators for the SPC/E water model. It is seen that for the chosen values of χ^{NR}_{xxz}, no major changes are observed in the overall features of the intensity profile. We also note that, at present, the value of the nonresonant component is not calculated from simulations[16] and its value is provided as an input into the calculations. The precise value of χ^{NR}_{xxz} including its sign is yet to be determined from theoretical calculations.

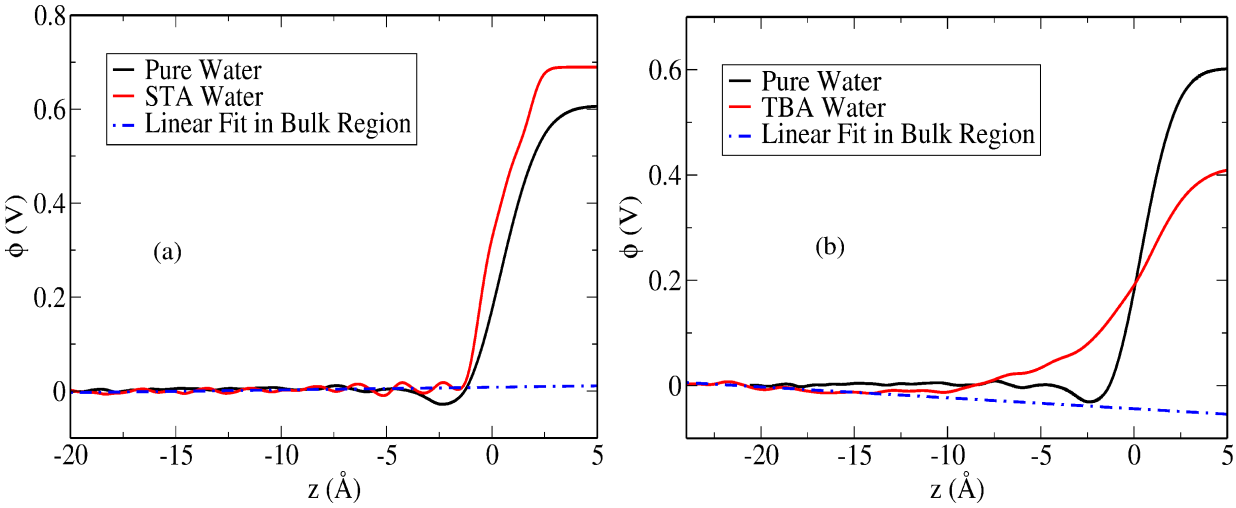

Figure S9: Variation of the electric potential $\phi(z)$ with z for (a) STA-water, and (b) TBA-water systems for SPC/E model of water. The results for pure air-water interface are also shown.

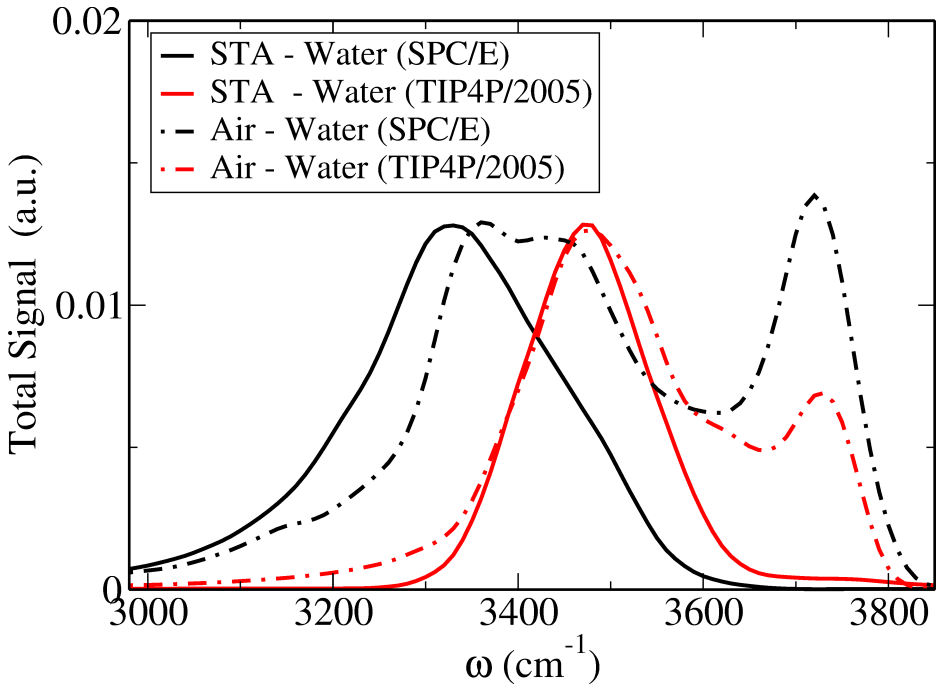

Figure S10: Intensity of VSFG signal of STA/water interface (solid curves) for SPC/E and TIP4P/2005 water models. The corresponding results for the pure air-water interface are also shown for the two water models (dashed curves).

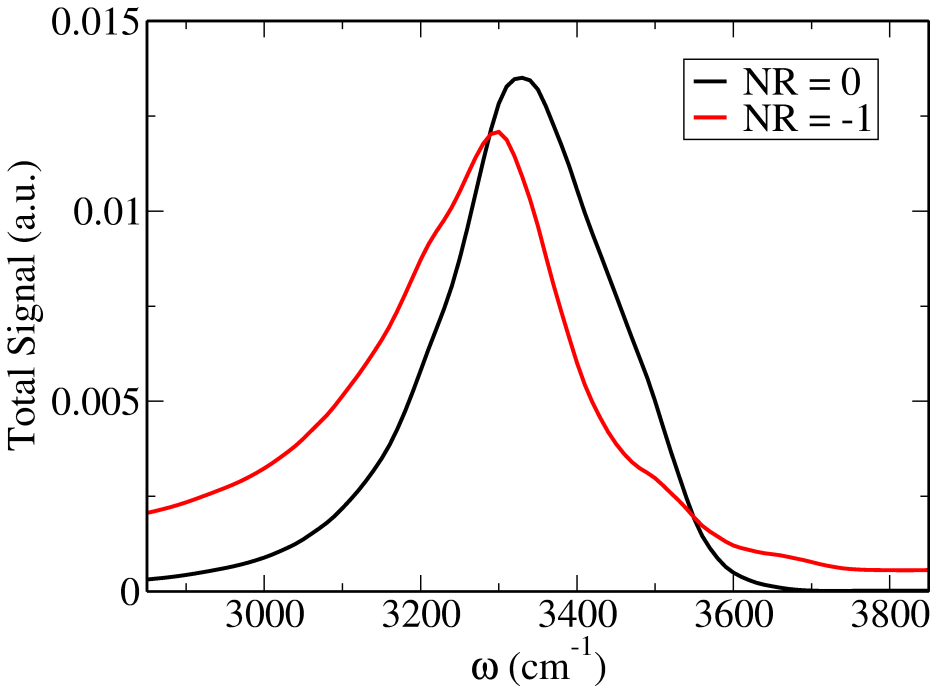

Figure S11: Intensity of VSFG signal of STA/water interface for $\chi^{NR}_{xxz} = 0$ and -1 (Eq.1). The results of this figure are obtained using the SPC/E water model.

References

[1] A. D. Becke, *J. Chem. Phys.*, 1993, **98**, 5648–5652.

[2] C. Lee, W. Yang and R. G. Parr, *Phys. Rev. B* 1988, **37**, 785-789.

[3] P. J. Stephens, F. J. Devlin, C. F. Chabalowski, M. J. Frisch, *J. Phys. Chem.* 1994, **98**, 11623-11627.

[4] M. J. Frisch, G. W. Trucks, H. B. Schlegel, G. E. Scuseria, M. A. Robb, J. R. Cheeseman, G. Scalmani, V. Barone, B. Mennucci, G. A. Petersson, et al *Gaussian 09*, Revision E.01; Gaussian Inc.: Wallingford, CT, 2009.

[5] A. P. Willard and D. Chandler, *J. Phys. Chem. B*, 2010, **114**, 1954–1958.

[6] J. L. Abascal and C. Vega, *J. Chem. Phys.*, 2005, **123**, 234505.

[7] B. Das, B. Sharma and A. Chandra, *J. Phys. Chem. C*, 2018, **122**, 9374–9388.

[8] D. R. Moberg, Q. Li, S. K. Reddy and F. Paesani, *J. Chem. Phys.*, 2019, **150**, 034701.

[9] S. Habershon, T. E. Markland, D. E. Manolopoulos, *J. Chem. Phys.* 2009, **131**, 024501.

[10] Y. -C. Wen, S. Zha, C. Tian and Y. R. Shen, *J. Phys. Chem. C*, 2016, **120**, 15224-15229.

[11] Y. -C. Wen, S. Zha, X. Liu, S. Yang, P. Guo, G. Shi, H. Fang, Y. R. Shen and C. Tian, *Phys. Rev. Lett.*, 2016, **116**, 016101.

[12] P. E. Ohno, H. F. Wang and F. M. Geiger, *Nature Commun.*, 2017, **8**, 1032–1040.

[13] T. Joutsuka, T. Hirano, M. Sprik and A. Morita, *Phys. Chem. Chem. Phys.*, 2018, **20**, 3040–3053.

[14] S. Pezzotti, D. R. Galimberti, Y. R. Shen and M. -P. Gaigeot, *Phys. Chem. Chem. Phys.*, 2018, **20**, 5190–5199.

[15] Q. Du, R. Superfine, E. Freysz and Y. R. Shen, *Phys. Rev. Lett.*, 1993, **70**, 2313–2316.

[16] F. Tang, T. Ohto, S. Sun, J. R. Rouxel, S. Imoto, E. H. G. Backus, S. Mukamel, M. Bonn and Y. Nagata, *Chem. Rev.* 2020, **120**, 3633-3667.